

# **Experimental study of the hydro-mechanical behaviour of a compacted lateritic sandy lean clay**

**Authors:** C. W. W. Ng, D. B. Akinniyi and C. Zhou\*

\* Corresponding author

**Author's affiliation and address:**

**Name:** Charles Wang Wai Ng

**Title:** CLP Holdings Professor of Sustainability

**Affiliation:** Department of Civil and Environmental Engineering, Hong Kong University  
of Science and Technology, Hong Kong

**Name:** Damilola Bashir Akinniyi

**Title:** Postdoctoral fellow

**Affiliation:** Department of Civil and Environmental Engineering, Hong Kong University  
of Science and Technology, Hong Kong

**Name:** Chao Zhou

**Title:** Assistant Professor

**Affiliation:** Department of Civil and Environmental Engineering, Hong Kong Polytechnic  
University, Hung Hom, Hong Kong

**Email:** [c.zhou@polyu.edu.hk](mailto:c.zhou@polyu.edu.hk)

## **Abstract**

Lateritic clay is widely distributed in tropical areas and extensively used as foundation materials. Compared to other soils, it is rich in iron and aluminum oxides (sesquioxide), which enhance the formation of soil aggregates. The principal objective of this study is to investigate the hydro-mechanical behaviour of a lateritic sandy lean clay. All specimens were compacted at the same condition and then wetted to a predefined suction (0, 50, 150 kPa). Suction-controlled isotropic compression and shear tests were carried out. Moreover, soil microstructures at various suctions were determined using the mercury intrusion porosimetry (MIP) and scanning electron microscope (SEM) techniques. The compressibility of the lateritic clay decreased by about 50% as suction decreased from 150 and 0 kPa. This is mainly because that as the suction decreased to 150 kPa, the sizes of inter-aggregate pores decreased as a result of the aggregate swelling, as revealed by MIP data. During shearing, the critical state friction angle appeared to be independent of suction. The contribution of suction to the apparent cohesion is unexpectedly low, likely because the inter-aggregate pores have low degree of saturation and the contribution of water meniscus on shear strength is very low.

**Keywords:** Aggregates, sesquioxide, microstructure, compressibility, critical state; lateritic soil

## **Introduction**

Lateritic clay is widely distributed in the humid tropical and subtropical regions e.g. South America (Brazil), West Africa (Nigeria) and Asia (India and China) (Gidigas, 1976). It is very different from other soils, because it has much higher content of iron and aluminum oxides (sesquioxide) and often contains some secondary minerals such as goethite and hematite (Ng et al., 2019a). The iron and aluminum oxides play an important role in the formation and stabilization of large-size aggregates (Schwertmann & Fitzpatrick, 1992; Larrahondo & Burns, 2013). Through microstructural analysis, some previous researchers (Ng et al., 2019a; Otalvaro et al., 2015; Futai & Almeida, 2005) have confirmed the presence of large-size aggregates in the lateritic clay. It is reasonable to postulate that the significant aggregation would alter the pore size distribution, water retention behaviour, compression and shear behaviour of unsaturated lateritic clay. Up to now, however, experimental studies on the unsaturated lateritic soil are very limited.

To investigate the shear behaviour of lateritic gravel, Toll (1990) compacted soil specimens at different water contents and then tested them. It was found that water content had significant influence on the measured shear strength. Futai & Almeida (2005) studied the compressibility and shear strength of an intact gneiss lateritic clay along a drying path through suction-controlled triaxial tests. They observed a significant increase in shear strength with increasing suction. In addition, Costa et al. (2003) reported the influence of suction on the

behaviour of an unsaturated lateritic soil through plate loading tests. Osinubi & Nwaiwu (2006) measured the shrinkage and unconfined compressive strength of a compacted lateritic soil at unsaturated condition. Their test results all demonstrated the importance of suction effects on lateritic soils. The above studies only investigated soil response at as-compacted state or during the drying path, although the excessive deformation and failure of lateritic soil usually occur during rainy season (Meshida, 2006; Gui & Yu, 2008). More importantly, it is well recognized that macro soil behaviour is greatly affected by its microstructures (Zhou and Ng, 2014; Ng et al., 2019b). Previous studies on other soils have revealed that the change in soil microstructure is more significant during the wetting process than that during the drying process (Delage et al. 1996; Koliji et al. 2000; Tarantino, 2011). The previous studies did not carry out microstructural analysis at various suctions to analyze the influence of sesquioxide on the microstructure and macro behaviour of unsaturated lateritic soil. Hence, it is necessary to study the mechanical behaviour and microstructures of lateritic clays along the wetting process.

In this study, two series of suction-controlled triaxial tests were designed and carried out to investigate the hydro-mechanical behaviour of a lateritic sandy lean clay. Suction effects on the yield stress, compressibility, dilatancy, peak and critical state strengths were determined and analysed. To provide insights to the measured macro behaviour, the evolution of soil microstructure along the wetting process was studied through MIP and SEM tests.

### **Test soil and specimen preparation**

The test soil was sampled from Nigeria, West Africa. There were many large-size aggregates in the block soil sample, and they were broken down using the free fall method (Ng & Chiu, 2003). To enhance the uniformity of a triaxial specimen, soil particles over 2 mm were discarded after sieving the soil through a 2 mm sieve size. Physical properties of the soil were determined following the ASTM standard (ASTM, 2011) and summarized in Table 1. The results from wet sieve and hydrometer particle size distribution shows that the soil contains 42% sand, 16% silt and 42% clay content. The values of the coefficient of uniformity and of gradation were estimated to be 35 and 1.6, respectively. The tested soil is considered to be well graded (ASTM D2487, 2011). According to the unified soil classification system (ASTM, 2011), the soil is classified as a sandy lean clay (CL).

The chemical composition in the soil was measured using the X-ray Fluorescence (XRF) technique. The iron oxide and aluminum oxide contents are 10% and 28%, respectively. Hence, the sesquioxide content is equal to 38%, which is about two times of that of a completely decomposed granite (CDG) (Ng et al., 2019a). The high sesquioxide content of lateritic soil is closely related to its formulation process, which involves the leaching of silica from the soil and leads to the accumulation of iron and aluminum oxides (Alexander and Cady, 1962).

Figure 1 shows the soil water retention curves (SWRC) of the compacted lateritic sandy lean clay measured using the one-dimensional pressure plate apparatus. SWRC of the lateritic sandy lean clay was determined using a one-dimensional pressure plate apparatus, which

controls soil suction using the axis-translation technique. The specimen was compacted in an oedometer ring and then placed on a saturated ceramic disk. During the test, the specimen was firstly saturated using the method proposed by Vanapalli et al. (1996). Then, the specimen was subjected to a drying and wetting cycle, by increasing and decreasing soil suction in the range of 0 to 400 kPa. At each suction stage, water flow rate and vertical deformation of the specimen were monitored using burette and dial gauge, respectively. When the water flow rate is less than  $0.81 \times 10^{-12} \text{ m}^3/\text{s}$  (Ng et al., 2016), it was assumed that the specimen had reached suction equalisation. It took 3–12 days for suction to reach equalization according to this criterion.

During the drying and wetting process from 0 to 400 kPa, the maximum vertical strain of the specimen was less than 1%. Moreover, the specimen was in good contact with the oedometer ring, suggesting that the lateral dimension of soil specimen remained almost constant (Ng et al., 2019c). It is therefore reasonable to assume that the volumetric strain is equal to the vertical strain.

From the SWRC, the air entry value (AEV) of the lateritic soil is estimated to be 1.8 kPa. This value is very low, compared with other types of clay. The low AEV of lateritic soils, which was also observed by Sun et al. (2016), indicate the presence of large inter-aggregate pores. It can also be observed that the SWRC shown is typical of a specimen having unimodal pore size distribution; although a bimodal pore size distribution is expected in the compacted lateritic sandy lean clay. This observation suggests that desaturation occurs only in the inter-

aggregate pores within the suction range of 0 and 200kPa. More discussion on the SWRC curve is given later while explaining the compressibility and shear behaviour.

In this study, the under compaction method proposed by Ladd (1978) was adopted to prepare soil specimens. All specimens were compacted at the same dry density ( $1.6 \text{ g/cm}^3$ ) and water content (19%) to ensure that all specimens have an identical microstructure after specimen preparation. The initial suction of each specimen was measured using the null technique. It was found that the initial suctions fell in the range of 150 to 160 kPa.

### **Suction-controlled triaxial apparatus**

The compression and shear tests were conducted using a GDS stress path triaxial system. The suction was controlled using the axis translation technique. A double cell system (Ng et al., 2002) was used for measuring the total volume change of unsaturated soil specimen. This system uses an accurate differential pressure transducer to record the changes in the differential pressure, which depends on the water levels inside a bottle-shaped inner cell and a reference tube. During a test, water level in the reference tube is maintained constant, while water level in the inner cell varies upon a volume change of soil specimen. The estimated accuracy of the double cell system is 0.04% of the measurement of volumetric strain. More details of the triaxial apparatus and the double cell system were reported by Ng et al. (2002) and Ng et al. (2009).

### **Test program and procedures**

Two series of triaxial tests were carried out on the compacted lateritic soils. The first series of tests was suction-controlled isotropic compression tests, designed to study the loading-collapse (LC) curve and suction effects on soil compressibility. Three suctions were considered: 0, 50 and 150 kPa. The second series was designed to study the influence of suction on the shear behaviour, including the dilatancy, peak and critical state strengths. Three suctions of 0, 50 and 150 kPa and three net confining pressures of 50, 100 and 200 kPa were adopted. Details of the triaxial tests are summarized in Table 2.

Figure 2 shows the stress path of all specimens. The initial state of soil specimens is denoted by point A in the figure. After soil specimen in the triaxial apparatus, a net confining pressure of 20 kPa was applied. Then, each specimen was wetted from the initial suction to a predefined suction (150, 50 and 0 kPa) following the stress path of  $A \rightarrow A_0 \rightarrow B_0 \rightarrow C_0$ . It took 5 to 7 days for the specimens to achieve the suction equalization. The equilibrium degree of saturation for the specimens at suctions of 0, 50 and 150 kPa are 98%, 87% and 79%, respectively. After suction equalization, the net confining pressure of each specimen was increased to the predefined value. For example, the stress path for the specimen LT150 was  $A_0 \rightarrow A_1 \rightarrow A_2 \rightarrow A_3$ . Following the method of Thomas (1987), the rate of ramped compression was selected to be 0.5 kPa per hour to minimize the excess pore water pressure. After the increase of net confining pressure, a time lapse of 24 hours was allowed for full dissipation of any excess pore water pressure. The saturated and unsaturated specimen were finally subjected



to drained and constant suction shearing (for example,  $A_1 \rightarrow A'_1$  for LT150-50), respectively. The rate of shearing was 0.003%/min, estimated from the equation proposed by Ho & Fredlund (1982). During the shearing process, the confining pressure was kept constant. The double cell system was used to monitor the total volume change, while a GDS back pressure controller was adopted to measure the water volume change of soil specimen.

To explain the results of suction-controlled triaxial, microstructure analysis was conducted based on the MIP and SEM tests. Three specimens were prepared in the same manner as those used in the triaxial tests. One of the specimens was directly used to for MIP and SEM tests, and the results represent the soil microstructure at a suction of 150 kPa. The other two specimens were wetted to 50 and 0 kPa respectively and then tested. By comparing the soil microstructures at various suctions, the effects of suction can be determined.

## **Interpretations of experimental results**

### *Soil compressibility at various suctions*

Figure 3 shows the measured isotropic compression curves at various suctions of 0, 50 and 150 kPa. A gradual change in specific volume with increasing net stress is first observed in each lateritic soil until a yield point. The yielding stresses (i.e., the preconsolidation pressure,  $p_c$ ) were estimated using the Casagrande's graphical method. The values of  $p_c$  are 80, 100 and 140 kPa at suctions of 0, 50 and 150 kPa respectively. After yielding, a much larger compressibility is observed in each specimen, and a post-yield isotropic normal compression

line (NCL) can be determined at each suction. The slope ( $\lambda$ ) and intercept (N) of the NCL were estimated and summarized in Table 3. At suctions of 0 and 50kPa, there seem no difference in the values of  $\lambda$ , suggesting that the compressibilities at these two suctions are almost the same. For the specimen at a suction of 150 kPa, it can be seen from the figure that the slope of its NCL becomes significantly larger than those at suctions of 0 and 50 kPa. The steeper NCL indicates that the specimen is more compressible at a suction of 150 kPa. Suction effects on the compressibility is closely related to the microstructure of lateritic soil. More discussion is given later.

At saturated state, the slope of the NCL ( $\lambda$ ) for the lateritic soil is lower than those of saturated kaolin clay (Wheeler & Sivakumar, 1995) and CDG (gravelly sand) (Chiu & Ng, 2003). The lateritic soil is thus less compressible than the other two soils. This is mainly because the lateritic soil consists of many large-size aggregate, as suggested by the low AEV of the lateritic soil (see Figure 1). The large-size aggregates can enhance the interlocking inside the soil specimen. As a result, the soil skeleton becomes more stable, leading to a lower compressibility.

Figure 4 shows the variation of  $\lambda(s)$  with suction for the lateritic sandy lean clay. To understand suction effect more clearly, the  $\lambda(s)$  at each suction were normalized with their respective saturated compressibility  $\lambda(0)$ . The value of  $\lambda(s)$  for the two replicated lateritic soils are very close, suggesting the measured results have a high repeatability. As explained

previously, the  $\lambda(s)$  of lateritic soil decreases sharply after wetting from 150 to 50 kPa suction and then fairly becomes constant at 0kPa. Similarly, the decrease of  $\lambda(s)$  with decreasing suction was also observed in kaolin clay (Wheeler & Sivakumar, 1995) and CDG, gravelly sand (Chiu & Ng, 2003). At a quantitative level, the decrease rate of  $\lambda(s)$  with decreasing suction is much larger in the lateritic sandy lean clay compared to those in the kaolin clay and CDG (gravelly sand). The decrease in the compressibility of the lateritic soil from a suction of 50 and 150 kPa is about 50%. The high compressibility of the lateritic soil at a suction of 150 kPa is mainly due to the presence of large-size inter-aggregate pores. More discussion based on the results of MIP tests is given later. On the other hand, this study shows that decreasing suction from 150 to 0 kPa can significantly decrease the compressibility of lateritic soil by about 50%.

#### *Loading collapse yield curve*

Figure 5 shows the initial location of the loading collapse (LC) yield curve for the lateritic sandy lean clay, prior to the application of compression and wetting. This curved was determined by using the preconsolidation pressures ( $p_c$ ) obtained from Figure 3. The initial states of all specimens prior to constant-suction shearing are also shown in this figure for comparisons. From the figure, it can be seen that the LC yield curve for the lateritic sandy lean clay is almost linear within the suction range studied. As suction decreases from 150 to 0 kPa, the preconsolidation pressure decreases from 140 to 80 kPa. The significant influence of

suction on the preconsolidation is mainly because the meniscus water is able to stiffen soil skeleton.

#### *Stress-strain relations during the shearing process*

Figure 6a shows the stress-strain curve of the lateritic soils sheared at various suctions (0, 50 and 150 kPa) and confining pressures (50, 100 and 200 kPa). For the specimens at 0 and 50 kPa suction sheared at 50 kPa net stress, a strain hardening behaviour is observed with no evidence of peak. The saturated specimen approaches a plateau while the specimen at 50 kPa suction is still showing significant change in deviator stress toward the end of the test. For the specimen at 150 kPa suction sheared at 50 kPa net stress, the deviator stress first reaches a peak at about 20% axial strain and then softens till the end of the test. At the end of the test, the deviator stress of the specimen at 150 kPa suction is still changing. The determination of the critical state line is discussed later.

For the six specimens sheared at 100 and 200 kPa net stress, all the specimen shows a strain hardening behaviour with no sign of peak or softening. A careful look into the figure shows that the contribution of suction to the deviator stress reduces with increasing net stress, mainly attributed to the high degree of saturation of the specimen before to shearing. After consolidation to 200 kPa, the degree of saturation at 50 kPa and 150 kPa suction is 91% and 89% respectively. It is reasonable to assume that the area covered by water is larger than the area of air. Moreover, as suggested by SWRC in Figure 1, the changes in degree of saturation

during wetting from 150 kPa and 50 kPa is quite low. Therefore, the presence of several saturated packet reduces the contribution of suction to the apparent cohesion component of the shear strength.

#### *Shearing-induced dilatancy*

Figure 6b shows the volume change of the lateritic soil during shearing at various suctions and net confining pressures. At zero suction, all specimens showed contraction behaviour throughout the shearing process and the contractive strain increased with increasing net confining pressure. This is because all specimens at zero suction are normally consolidated or slightly over-consolidated, as shown in Figure 5. For the unsaturated specimens at 50 and 150 kPa suctions sheared at 50 kPa net stress, contraction is first observed until about 10% axial strain followed by dilation till end of the test. The initial contraction behaviour of the unsaturated specimens is attributed to collapse of some unstable large-size inter-aggregate pores. The dilation behaviour is attributed to the rearrangement of soil aggregates with an over consolidation ratio larger than 2 (see Figure 5). As expected, the specimen at 150 kPa suction dilates more than the specimen at 50 kPa due to higher over consolidation ratio.

For the unsaturated specimens at 50 and 150 kPa suctions sheared at 100 kPa net confining pressure, it can be seen that the dilation is slightly significant at 50 kPa suction than at 150 kPa suction, even though the specimen at 50 kPa have a lower over consolidation ratio. The higher dilatancy at 50 kPa suction may be explained using the compression behaviour shown in Figure

3. During the shearing process, the mean net stress of both specimens increased from 100 kPa. The compressibility at a suction of 150 kPa is larger than that at 50 kPa. As a result, the contractive volumetric strain is higher at a suction of 150 kPa.

At 200 kPa net stress which is more their initial yield stress (see Figure 5), the state of both specimens at 200 kPa confining stress lies on their NCL. In this region, the specimen at 50 kPa suction is significantly less compressible than at 150 kPa suction. As a result, the dilatancy behaviour of the lateritic soil at initial suction of 150 kPa is significantly suppressed by its highly compressible structure (see Figure 3). The results in this study are considered useful in the ultimate limit state design of earth structures built on lateritic soil, most especially in Africa. Compared to most unsaturated soil, the dilatancy behaviour observed in this study before and after their initial yield curve is not commonly observed. The findings from this study further confirms the dependence of soil dilation behaviour on the state of the specimen (Chiu & Ng, 2003). Similarly, dilation behaviour have been reported by Toll (1990) for a compacted lateritic gravel at high degree of saturation. Ng et al. (2019a) and Futai et al. (2004) on a loosely compacted lateritic sandy lean clay at saturated state also observed phase transformation from contraction to dilation. The presence of large sized particles in the lateritic soil increased the dilation tendency of the soil due to significant interlocking.

*Critical state of unsaturated lateritic soil*

In the current study, the ‘critical state’ parameters were consistently determined and assumed at an axial strain of 25%, where the deviator stress and volumetric strain have approached their respective asymptotic values. From the stress-strain curves shown in Figures 6a, the stress condition ( $p$ ,  $q$ ) of unsaturated specimens LT50-50 and LT150-50 did not fully reach the critical state. For other specimens, the rates of change in deviator stress were almost negligible at the end of the test. It is therefore reasonable to assume that these specimens have reached the critical state. Hence, the stress condition at the end of shearing may be used to approximate that at the critical state. On the other hand, it can be seen from Figures 6b that most of the unsaturated specimens were still dilating significantly at the end of shear tests. The critical state lines in the  $v$ - $\ln p$  plane cannot be determined accurately and hence are not shown in this study.

Figure 7 shows the critical state lines of the lateritic soils in the  $p$ - $q$  plane. A critical state line (CSL) is determined at each suction. The critical state strength envelope is drawn by fitting the data points using a straight line with a minimum  $R^2$  ( $R^2 = 0.9942, 0.9639$  and  $0.975$  at 0, 50 and 150 kPa, respectively). The CSLs at the three suctions were almost parallel, suggesting that suction does not affect the slope of the CSL within the suction range considered. The values of slope of the CSL,  $M(s)$  and the intercept  $\mu(s)$  are estimated and summarized in Table 3.

Figure 8a shows the variation of critical state stress ratio  $M(s)$  with suction, for the lateritic sandy lean clay. At the saturated state, the critical state stress ratio of the lateritic soil is larger

than that of a CDG, gravelly sand (Chiu & Ng, 2003), suggesting that the lateritic soil has a higher friction angle. The higher friction angle of the lateritic soil is attributed to the presence of large aggregates, which enhance the interlocking of aggregates and stabilize soil skeleton. Furthermore, it can be seen that the values of  $M(s)$  for the lateritic soil are not influenced by suction. The constant value of  $M(s)$  is consistent with the assumption in many unsaturated soil models (e.g., Alonso et al., 1990). For the test results of other lateritic soils, Toll (1990) reported an increasing  $M(s)$  with suction for a lateritic gravel. However, the maximum axial strain reached in Toll (1990) is 16%, which may not have brought the specimen to critical state. Furthermore, Futai & Almeida (2005) also reported an increasing  $M(s)$  with suction on an intact lateritic sandy lean clay. Even though 25% axial strain was reached in Futai & Almeida (2005), it is still not certain if critical state has been reached. This is because the compacted specimen used in this study did not fully reach the critical state at about 25% axial strain. Compared to the intact specimen tested by Futai & Almeida (2005), the structure of intact specimen is much more complex than a compacted specimen and may require shearing to larger axial strain. Therefore, the different fabric created in each specimen may influence the reported  $M$ . Furthermore, using extended Mohr Coulomb approach, Gui & Yu (2008) observed a constant friction angle for a compacted highly plastic lateritic sandy clay between suction of 0kPa and 160kPa. The results by Gui & Yu (2008) is similar to the variation of  $M(s)$  observed in this study.



Figure 8b shows the variation between the intercept,  $\mu$  (s), of the CSL and suction for lateritic sandy lean clay. The parameter  $\mu$ (s) indicates the contribution of suction to the shear strength of a soil. A linear decrease in  $\mu$  (s) with suction is observed. It can be seen that  $\mu$  (s) first decreases from 50 kPa at 150 kPa suction to about 25 kPa at 50 kPa suction. This 50% decrease in contribution of suction to shear strength is consistent with the observation observed in the compressibility (see Figure 4). The initial degree of saturation of the specimen after compaction, which is about 79%, may limit the effect of suction due to presence of several saturated aggregates.

#### *Suction effects on the microstructure of lateritic soil*

Figure 9a shows the SEM images of the lateritic soil at a suction of 150 kPa. Some inter-aggregate pores, with a diameter up to 100  $\mu\text{m}$ , are observed. Fine clay particles are almost invisible, even though the clay content of the lateritic soil is up to 42%. This is mainly because clay particles have coated the sand particles to form large sized aggregates due to the influence of sesquioxides, which enhance the formation of soil aggregates (Zhang et al., 2016). Ng et al. (2019a) compared the aggregate sizes of the lateritic sandy lean clay with those in the CDG, which have a lower sesquioxide content. They found that aggregate sizes of the lateritic sandy lean clay are about 100% larger than those in the CDG.

At a suction of 150 kPa, the pores between aggregates are indicated in the figure and maximum inter-aggregate pore diameter was about 105 $\mu\text{m}$ . The maximum diameter reduced

to about 85  $\mu\text{m}$  after wetting from 150 to 50 kPa, as shown in Figure 9b. Furthermore, the inter-aggregate pores at zero suction (Figure 9c) were too small to be identified at the same magnification (i.e., x200), suggesting that the pore diameter reduced significantly. The observations from the SEM images as shown in the Figure 9 are also supported by the MIP results, which show that the diameter of inter-aggregate pores reduced due to wetting.

The results of SEM images can be used to explain the hydro-mechanical behaviour of the lateritic sandy lean clay. For example, soil specimens at a suction of 150 kPa have the largest inter-aggregate pores. Hence, the soil compressibility is the highest at a suction of 150 kPa (see Figure 3).

Figure 10a shows the volume of intruded voids in the MIP test. The difference between intruded void ratio and actual void ratio is the unintruded void ratio, which is induced by the limitation of MIP tests. The unintruded pores consist of three parts: pores larger than 200  $\mu\text{m}$ , pores smaller than 0.007  $\mu\text{m}$  and closed pores. Furthermore, the boundary between the intra-aggregate and inter-aggregate pores is at a diameter of about 0.3  $\mu\text{m}$ . Based on these results, the intruded inter-aggregate and intra-aggregate pores are determined and summarized in Table 4.

Figure 10b shows the differential pore volume of the lateritic sandy lean clay at suctions of 150, 50 and 0 kPa. All of the specimens exhibit dual-porosity structure, as indicated by the two major peaks, corresponding to inter-aggregate and intra-aggregate pores respectively. The

boundary between the intra-aggregate and inter-aggregate pores is at a diameter of about 0.3  $\mu\text{m}$ . Using the capillary law by Sun et al. (2016), the suction required to start to desaturate the intra-aggregate pores at 0.3  $\mu\text{m}$  is estimated as 860 kPa, which is the suction range of 0-400 kPa considered in the current study. Hence, only the inter-aggregate pores are desaturated and this is why the SWRC shown in Fig. 1 did not show a bimodal feature.

At a suction of 150 kPa, the peak value for the intra-aggregate pores are found at a diameter of 0.025  $\mu\text{m}$ , while the peak within the inter-aggregate zone is found at 120  $\mu\text{m}$ . The difference between intra-aggregate and inter-aggregates pores of this specimen is up to three orders of magnitude. Compared to published data on various compacted soils, this difference between inter-aggregate and intra-aggregate pores is remarkably high. For instance, Li & Zhang (2009) studied compacted CDG (at a condition with similar water content and dry density as the lateritic sandy lean clay), the difference between the two dominate pore sizes was only about one order of magnitude. This large difference between the intra-aggregate and inter-aggregate pores in the lateritic sandy lean clay indicates the presence of large-size pores, which are due to the large size of its aggregates (see Figure 9a, b &c).

Furthermore, it can be seen that the peak value within the inter-aggregate zone shifts from 120  $\mu\text{m}$  at 150-kPa suction to 70  $\mu\text{m}$  after wetting to 50 kPa suction. At zero suction, it can be observed that the diameter of the dominating inter-aggregate pores have reduced to 30  $\mu\text{m}$ . The reduction in the diameter of peak pore suggests that wetting lead to the collapse of some large

inter- aggregate pores. Moreover, this change in the inter-aggregate pore size is consistent with the observation from the SEM images shown in Figure 9.

### **Summary and conclusions**

The hydro-mechanical behaviour of a sandy lean clay lateritic soil was studied along a wetting path. Data from the isotropic compression and constant-suction shearing tests were provided and interpreted using the extended critical state framework for unsaturated soils. Microstructural evidence was used to explain the changes in microstructure due to wetting. The key findings are summarized as follows:

As suction was decreased from 150 to 0 kPa, the compressibility of the lateritic clay decreased by about 50%. This is mainly because as suction decreased to 0 kPa, the shrinkage of the aggregates reduced the inter-aggregate pores, as revealed by the results of MIP tests. The compression behaviour at 150 kPa suction may be specific to the initial testing condition considered in this study. This high compressibility at initial suction of 150 kPa can pose great threat to the serviceability of earth structures built on similarly compacted lateritic clays.

During shearing, strain softening was observed for the lateritic clay at a suction of 150 kPa and a net confining pressure of 50 kPa. All other specimens, with a higher confining pressure and/or a lower suction, showed a response of strain hardening. This is mainly because as suction decreased and confining pressure increased, the dilatancy becomes smaller.

The critical state friction angle of the lateritic clay was found to be independent of suction. The apparent cohesion decreases linearly as suction decrease. The contribution of suction to the apparent cohesion is unexpectedly low despite the high initial degree of saturation of the lateritic specimen. This is likely because most water in the lateritic soil is within the large-sized aggregates, while the inter-aggregate pores are in the residual zone.

The lateritic specimen maintains the bimodal pore size distribution (inter-aggregate and intra-aggregate pores) at 150 kPa suction till saturated condition. The bimodal PSD of the lateritic specimen at saturated condition is not consistent with the commonly reported unimodal PSD of fine-grained soils at saturated condition. The behaviour of the lateritic specimen indicates that the inter-aggregate pores did not collapse completely as commonly observed in most fine-grained soils. The skeleton of lateritic soil is stable due to the cementing effects of its 38% sesquioxide content.”

### **Acknowledgements**

The authors would like to acknowledge the financial supports provided by the Research Grants Council of the Hong Kong Special Administrative Region (HKSAR) through the research grants 16207918, 16216116 and AoE/E-603/18.

### **References**

Alexander, L. T., & Cady, J. G. (1962). *Genesis and hardening of laterite in soils* (Vol. 1281). US Dept. of Agriculture.

- Alonso, E. E., Gens, A., & Josa, A. (1990). A constitutive model for partially saturated soils. *Géotechnique*, 40(3), 405-430.
- ASTM D2487 (2011). Standard Practice for Classification of Soils for Engineering Purposes (USCS). American Society of Testing and Materials, West Conshohocken, PA.
- Chiu, C. F. (2001). *Behaviour of unsaturated loosely compacted weathered materials* (Doctoral dissertation). *Hong Kong University of Science and Technology*.
- Chiu, C. F., & Ng, C. W. W. (2003). A state-dependent elasto-plastic model for saturated and unsaturated soils. *Géotechnique*, 53(9), 809-829.
- Costa, Y. D., Cintra, J. C., & Zornberg, J. G. (2003). Influence of matric suction on the results of plate load tests performed on a lateritic soil deposit. *Geotechnical Testing Journal*, 26(2), 219-227
- Delage, P. (2009). DISCUSSION: Compaction behaviour of clay. A. TARANTINO and E. DE COL (2008). *Géotechnique* 58, No, 3, 199–213. *Géotechnique*, 59(1), 75-77.
- Delage, P., Audiguier, M., Cui, Y.J. & Howat, M.D. (1996). Microstructure of a compacted silt. *Canadian Geotechnical Journal*, 33: 150–158.
- Futai, M. M., & Almelda, M. S. S. (2005). An experimental investigation of the mechanical behaviour of an unsaturated gneiss residual soil. *Géotechnique*, 55(3), 201-214.
- Futai, M. M., Almeida, M. S. S., & Lacerda, W. A. (2004). Yield, strength, and critical state behavior of a tropical saturated soil. *Journal of Geotechnical and Geoenvironmental Engineering*, 130(11), 1169-1179.
- Gidigas, M.D. (1976). *Laterite Soil Engineering. Pedogenesis and Engineering Principles*. Elsevier, Amsterdam, pp. 535.
- Gui, M. W., & Yu, C. M. (2008). Rate of strength increase of unsaturated lateritic soil. *Canadian Geotechnical Journal*, 45(9), 1335-1343.

- Ho, D. Y., & Fredlund, D. G. (1982). A multistage triaxial test for unsaturated soils. *Geotechnical Testing Journal*, 5(1/2), 18-25.
- Koliji, A., Vulliet, L. & Laloui, L. (2010). Structural characterization of unsaturated aggregated soils. *Canadian Geotechnical Journal*, 47: 297–311.
- Ladd, R. S. (1978). Preparing test specimens using under-compaction. *Geotechnical Testing Journal*, 1(1), 16-23.
- Larrahondo, J. M., & Burns, S. E. (2013). Laboratory-prepared iron oxide coatings on sands: surface characterization and strength parameters. *Journal of Geotechnical and Geoenvironmental Engineering*, 140(4), 04013052.
- Li, X., & Zhang, L. M. (2009). Characterization of dual-structure pore-size distribution of soil. *Canadian Geotechnical Journal*, 46(2), 129-141.
- Meshida, E. A. (2006). Highway failure over talc–tremolite schist terrain: a case study of the Ife to Ilesha highway, South Western Nigeria. *Bulletin of Engineering Geology and the Environment*, 65(4), 457-461.
- Ng, C. W. W., Akinniyi, D. B., Zhou, C., & Chiu, C. F. (2019a). Comparisons of weathered lateritic, granitic and volcanic soils: Compressibility and shear strength. *Engineering Geology*, 249, 235-240.
- Ng, C. W. W., and Chiu, A. C. F. (2003). Laboratory Study of Loose Saturated and Unsaturated Decomposed Granitic Soil. *Journal of Geotechnical and Geoenvironmental Engineering*, ASCE, vol. 129, No. 6, pp 550–559.
- Ng, C. W. W., Mu, Q. Y. and Zhou, C. (2019b). Effects of specimen preparation method on the volume change of clay under cyclic thermal loads. *Géotechnique*, 68(12): 146–150.
- Ng, C. W. W., Owusu, S.T., Zhou, C. and Chiu, C.F (2019c). Effects of Sesquioxides Content on Stress-Dependent Water Retention Behaviour Weathered Soils. *Engineering Geology* (accepted)

- Ng, C. W. W., Sadeghi, H., Hossen, S. B., Chiu, C. F., Alonso, E. E., & Baghbanrezvan, S. (2016). Water retention and volumetric characteristics of intact and re-compacted loess. *Canadian Geotechnical Journal*, 53, (8), 1258-1269.
- Ng, C. W. W., Xu, J., and Yung, S. Y. (2009). Effects of wetting–drying and stress ratio on anisotropic stiffness of an unsaturated soil at very small strains. *Canadian Geotechnical Journal*, 46(9), 1062-1076.
- Ng, C. W., Zhan, L. T., & Cui, Y. J. (2002). A new simple system for measuring volume changes in unsaturated soils. *Canadian Geotechnical Journal*, 39(3), 757-764.
- Osinubi, K. J., & Nwaiwu, C. M. (2006). Design of compacted lateritic soil liners and covers. *Journal of geotechnical and geoenvironmental engineering*, 132(2), 203-213.
- Otalvaro, I.F., Neto, M.P.C., & Caicedo, B. (2015). Compressibility and microstructure of compacted laterites. *Transportation Geotechnics* 5, 20–34.
- Schwertmann, U. and Fitzpatrick, R.W. (1992). Iron Minerals in Surface Environments. *Oatena Supplement, Vol. 21, pp. 7-30.*
- Sun, D.A, Gao, Y., Zhou A.N., & Sheng D.C. (2016). Soil-water retention curves and microstructures of undisturbed and compacted Guilin lateritic clay. *Bulletin of Engineering Geology and the Environment*, 75(2): 781-791.
- Tarantino, A. (2011). Unsaturated soils: compacted versus reconstituted states. *Unsaturated soils. Edited by EE Alonso and A. Gens. CRC Press, Barcelona, Spain*, 113-136.
- Thomas, S. D. (1987). The consolidation behaviour of gassy soil. *PhD Thesis, University of Oxford.*
- Toll, D.G. (1990). A framework for unsaturated soils behavior. *Géotechnique* 40 (1), 31–44.
- Vanapalli, S. K., Fredlund, D. G., Pufahl, D. E., & Clifton, A. W. (1996). Model for the prediction of shear strength with respect to soil suction. *Canadian Geotechnical Journal*, 33(3), 379-392.



Wheeler, S. J., & Sivakumar, V. (1995). An elasto-plastic critical state framework for unsaturated soil. *Géotechnique*, 45(1), 35-53.

Zhang, X. W., Kong, L. W., Cui, X. L., & Yin, S. (2016). Occurrence characteristics of free iron oxides in soil microstructure: evidence from XRD, SEM and EDS. *Bulletin of Engineering Geology and the Environment*, 75(4), 1493-1503.

Zhou, C., and Ng, C. W. W. (2014). A new and simple stress-dependent water retention model for unsaturated soil. *Computers and Geotechnics*, 62, 216-222.

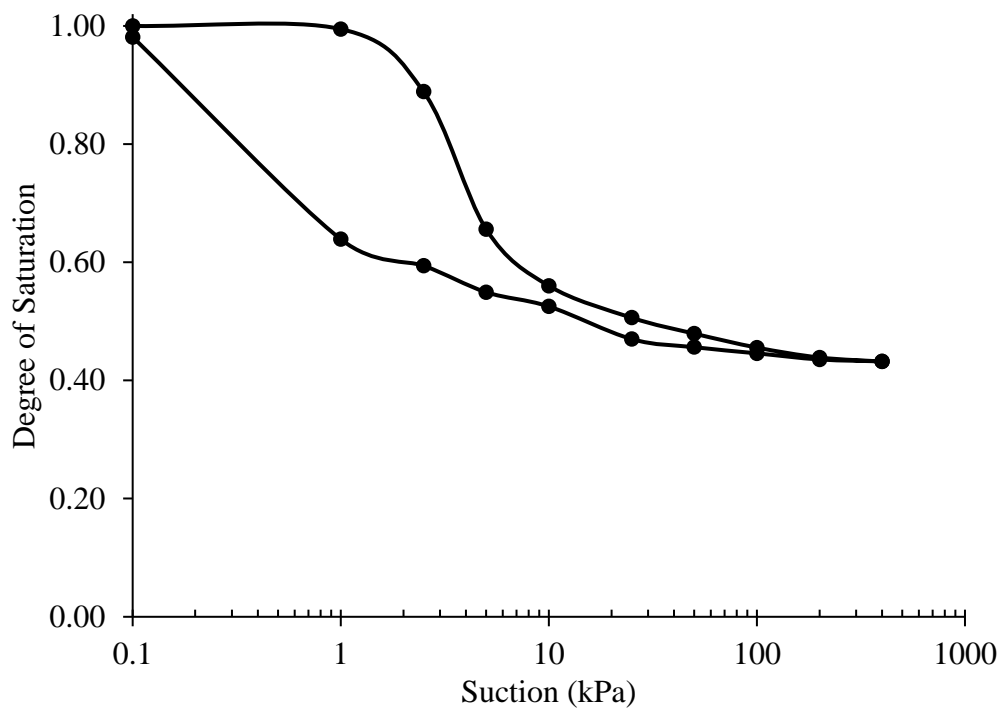


Fig. 1. Water retention curve of LAT tested in this study

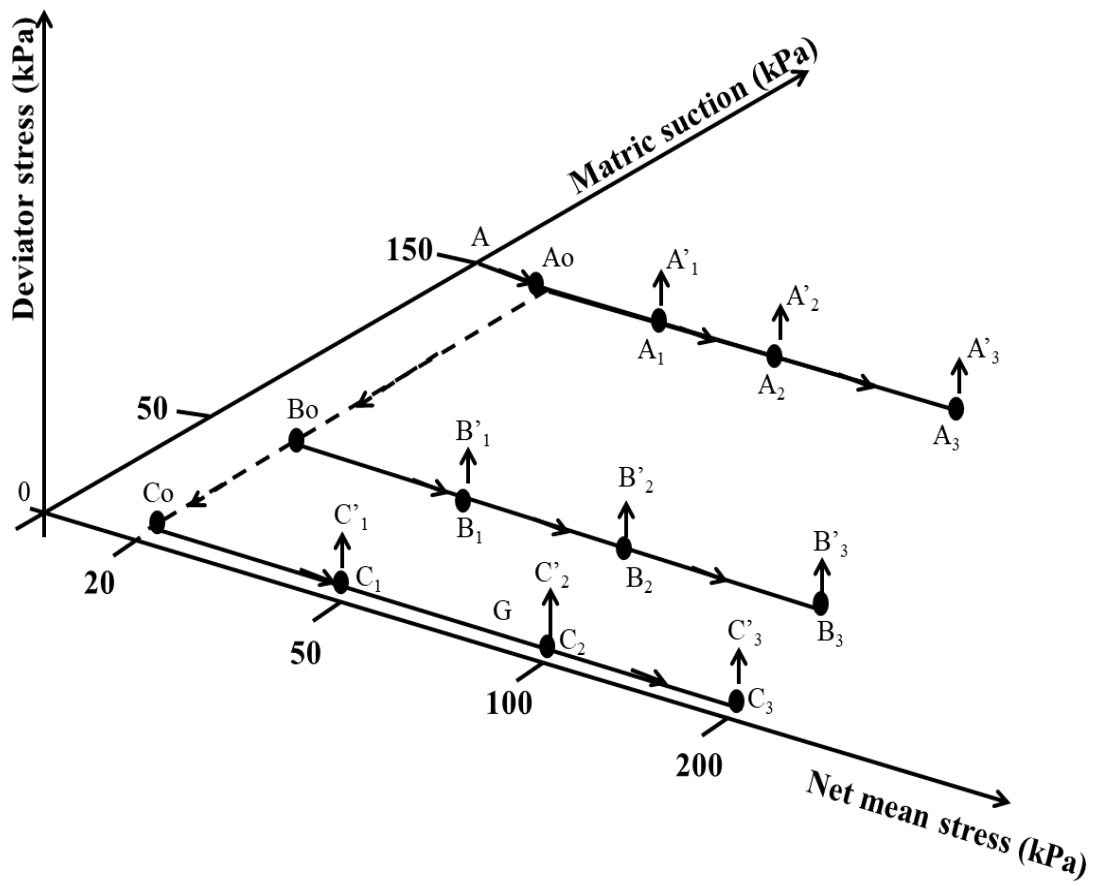


Fig. 2. Stress path during suction equalization, consolidation and constant-suction shearing

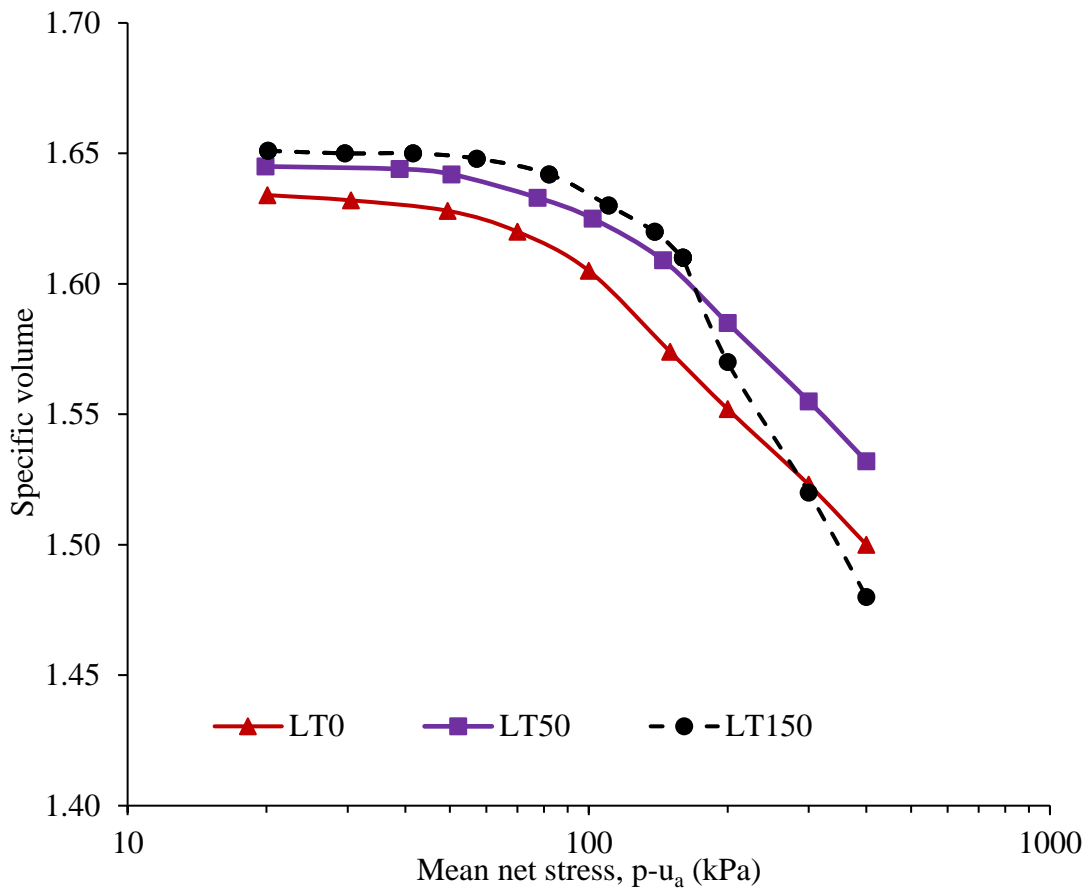


Fig. 3. Comparisons of isotropic compression behaviour of three different soils

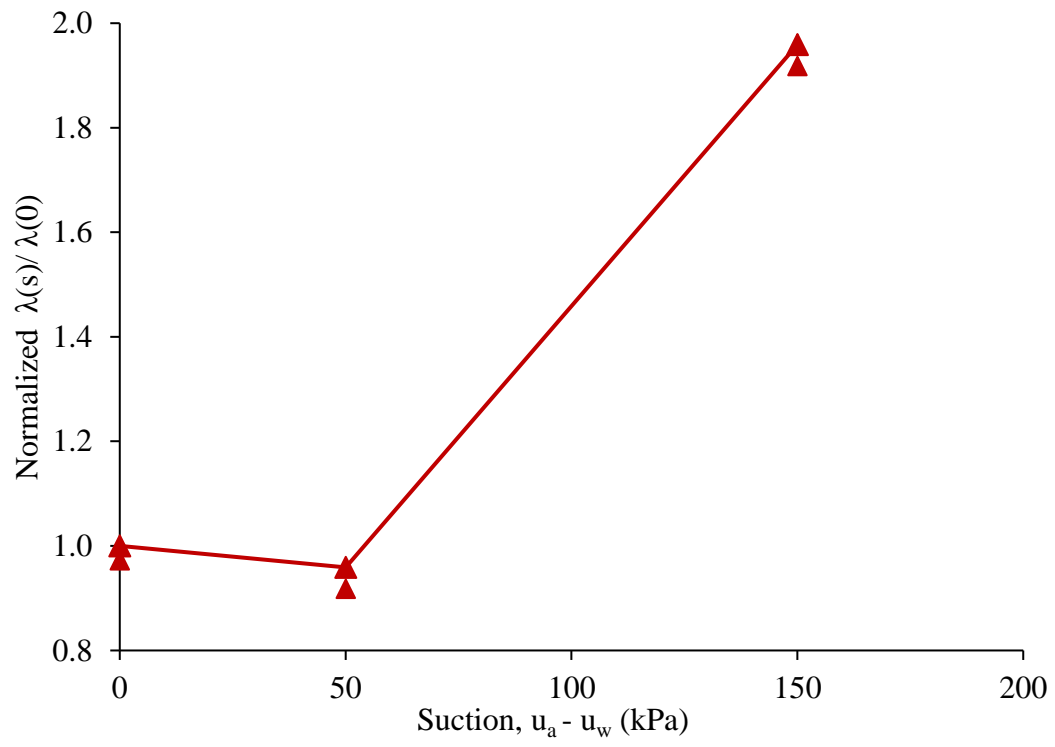


Fig. 4. Comparisons of compressibility variation with suction

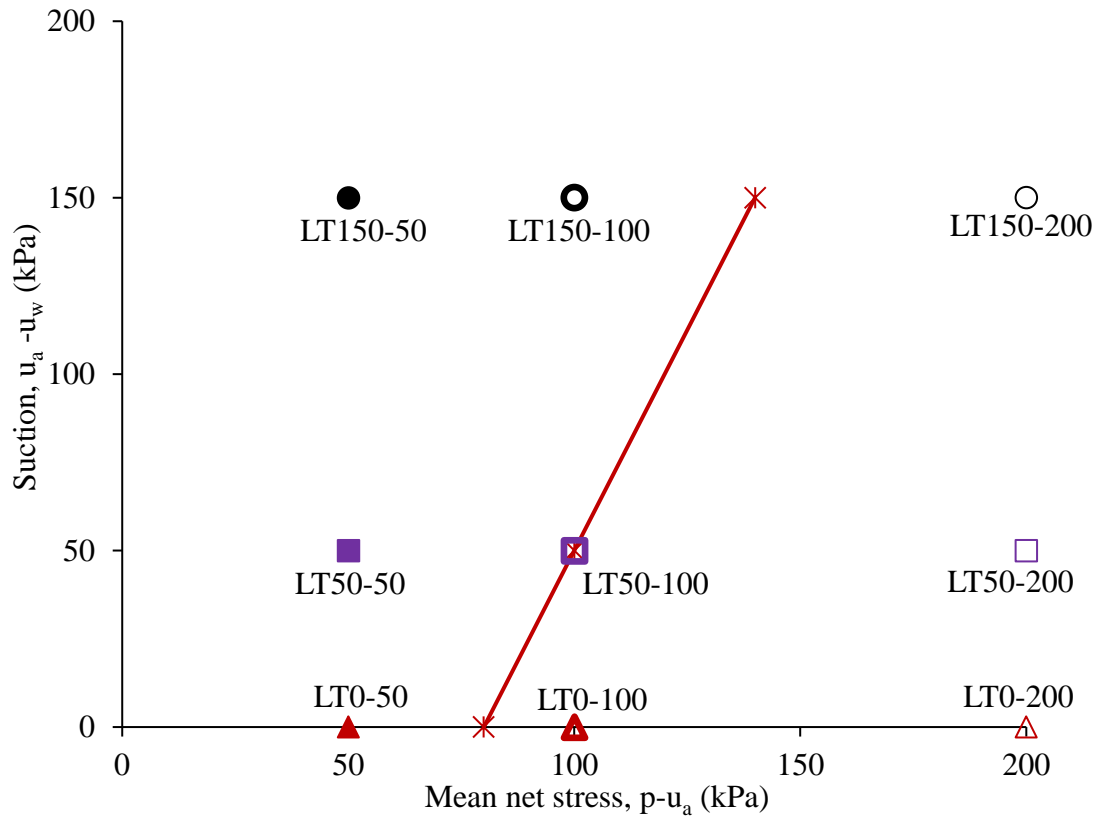
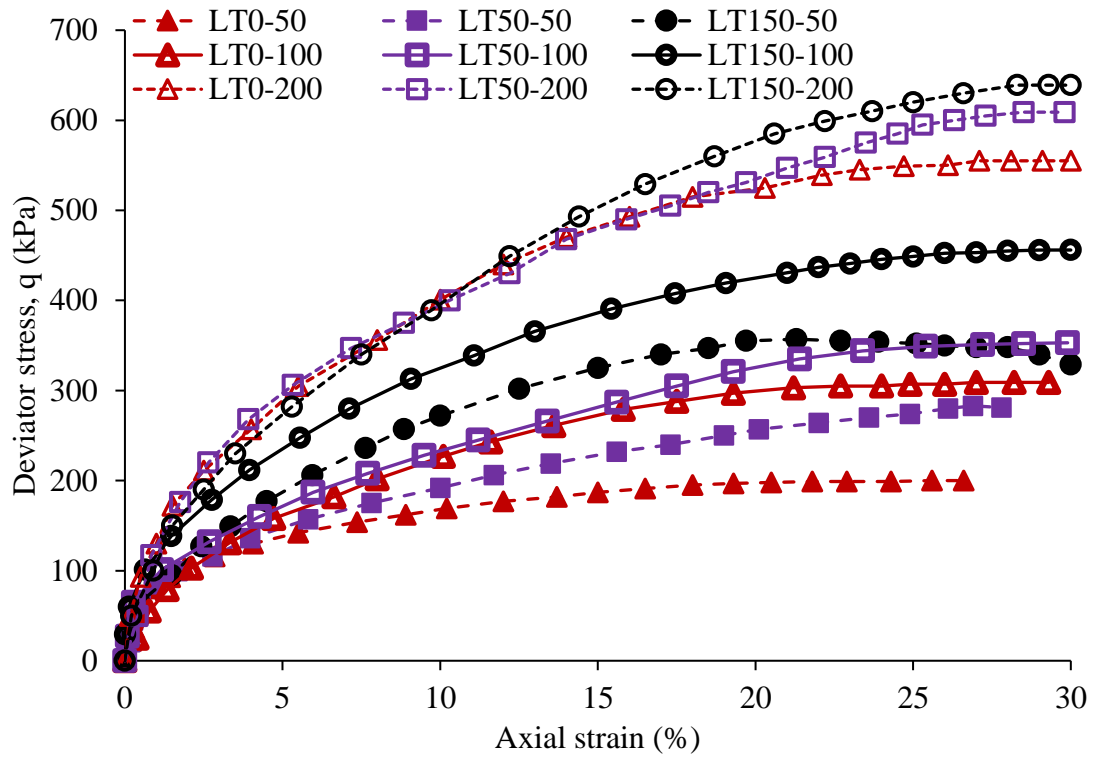
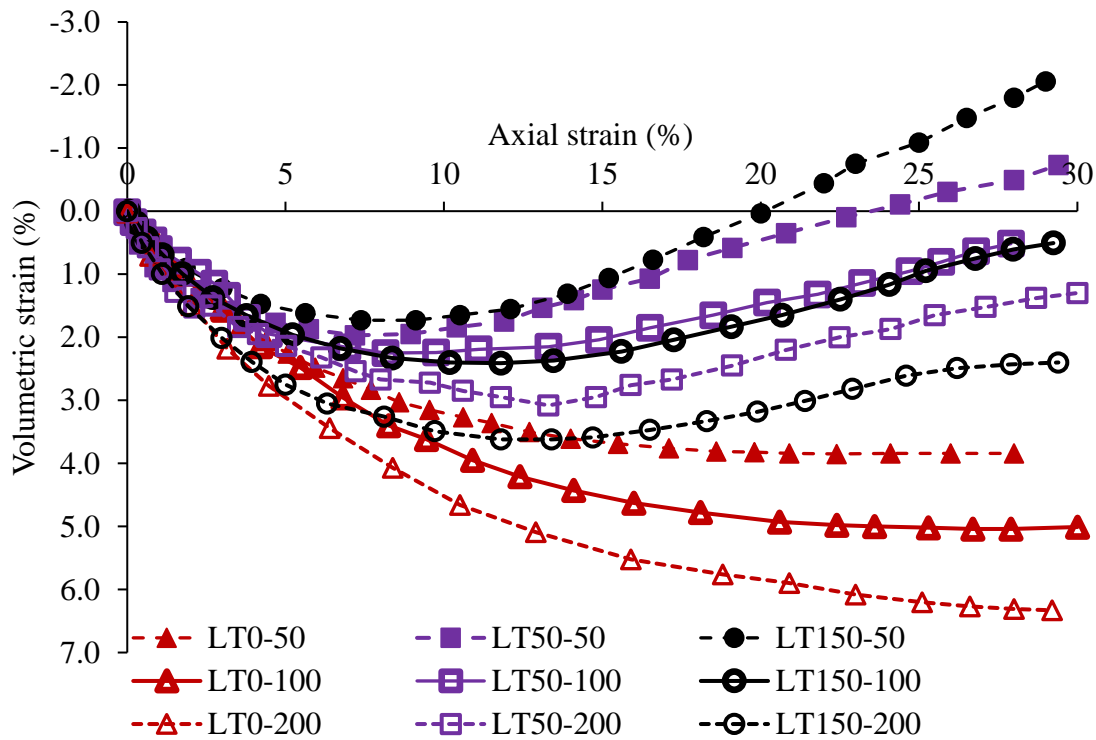


Fig. 5. The initial loading-collapse curve after specimen preparation and soil states prior to the shearing



(a)



(b)

Fig. 6. Results of constant-suction shearing tests behaviour of LAT at various suction and stressed: (a) stress-strain relations, (b) volume change against axial strain

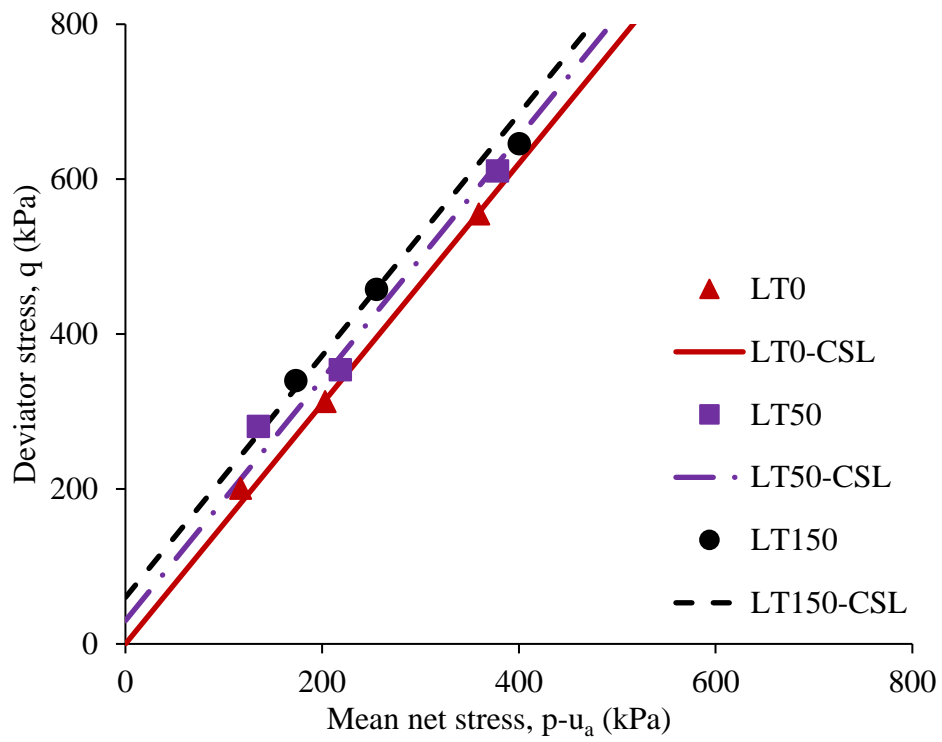
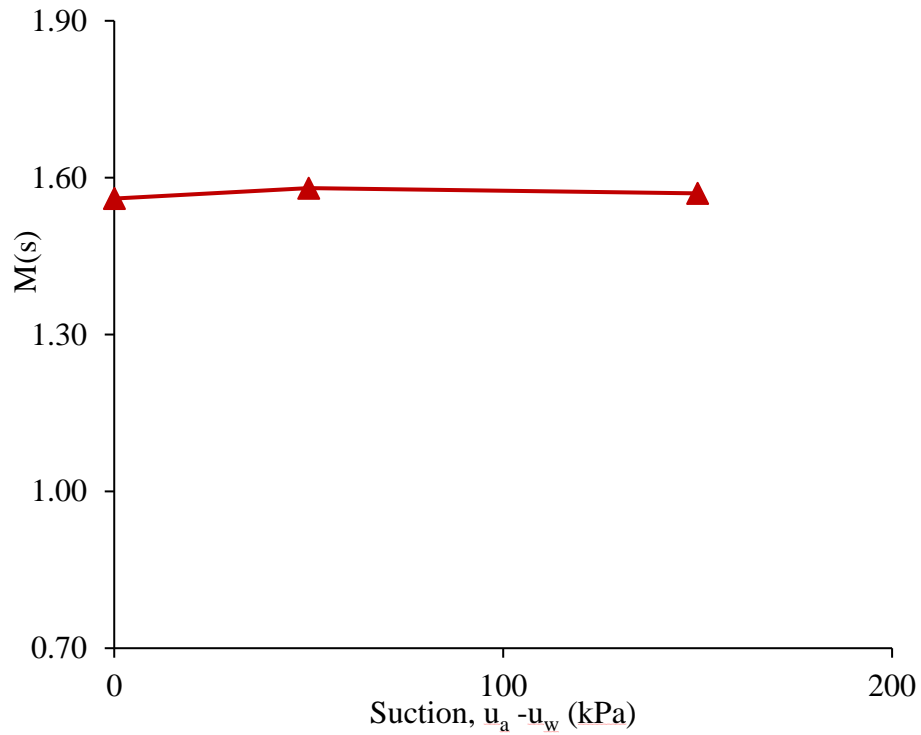
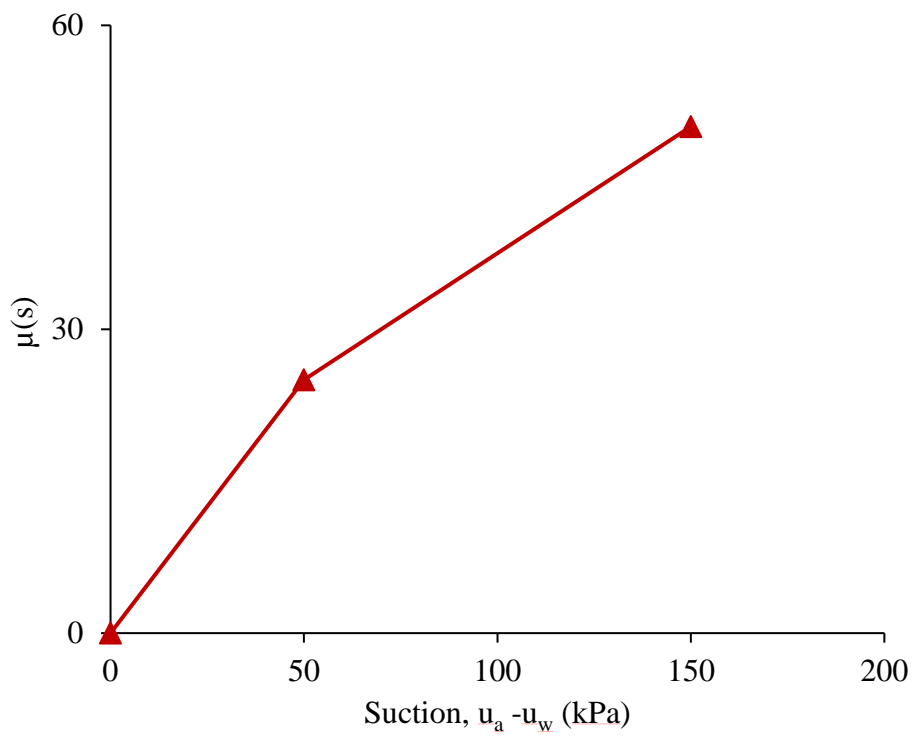


Fig. 7. Critical state strength envelope of LAT at various suctions (the three critical state lines are determined by fitting data points at each suction)



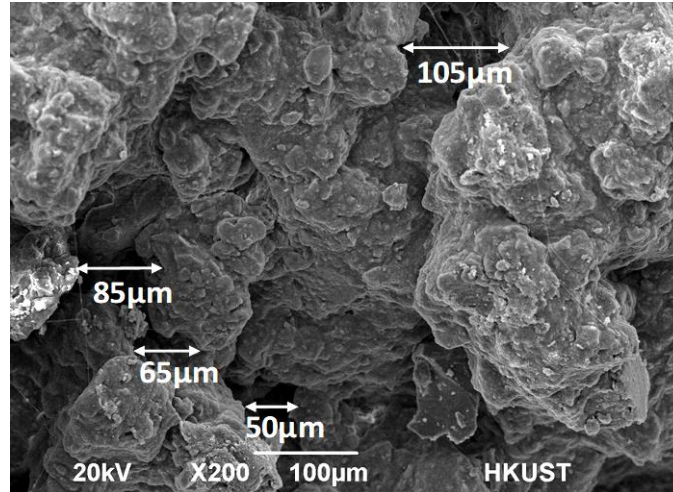


(a)

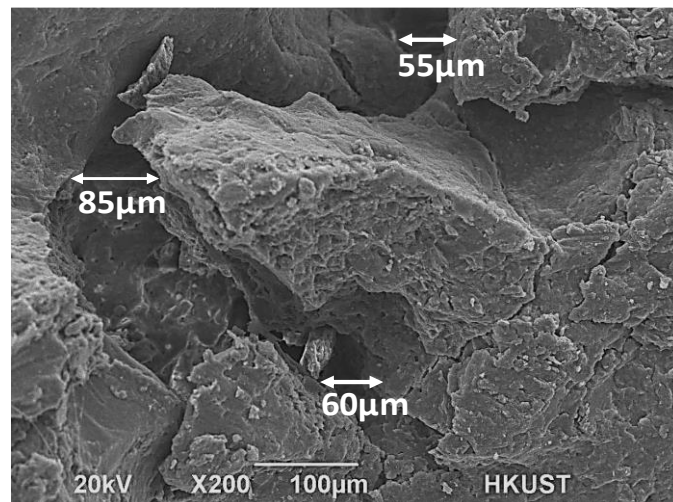


(b)

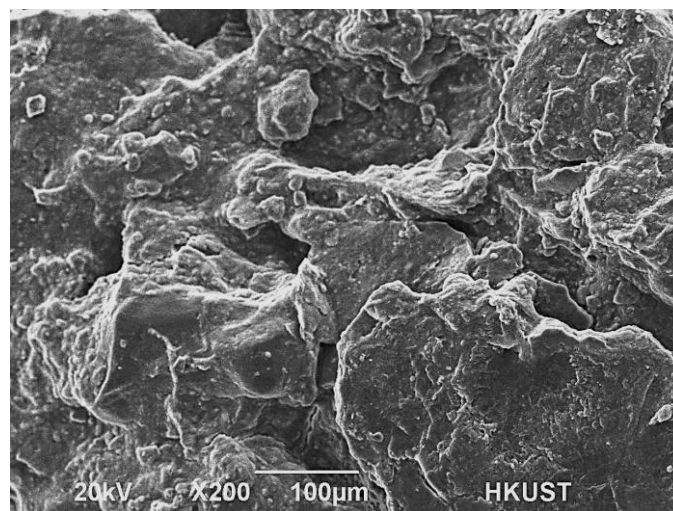
Fig. 8. Comparisons of suction effects on the critical state shear strength parameters a) critical state stress ratio, b) apparent cohesion



(a)

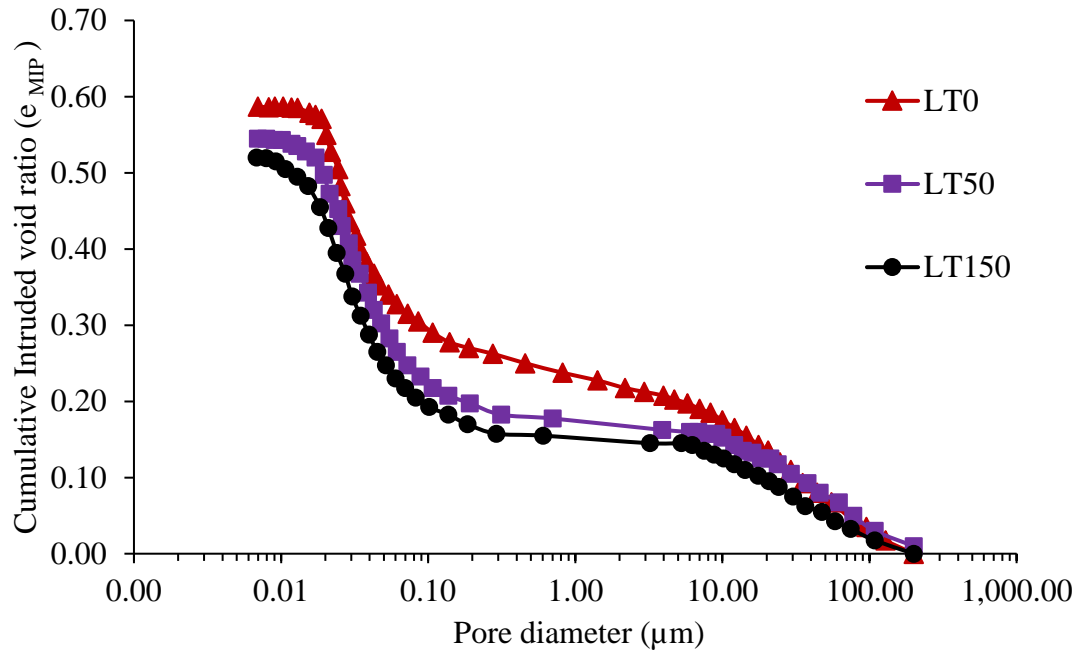


(b)

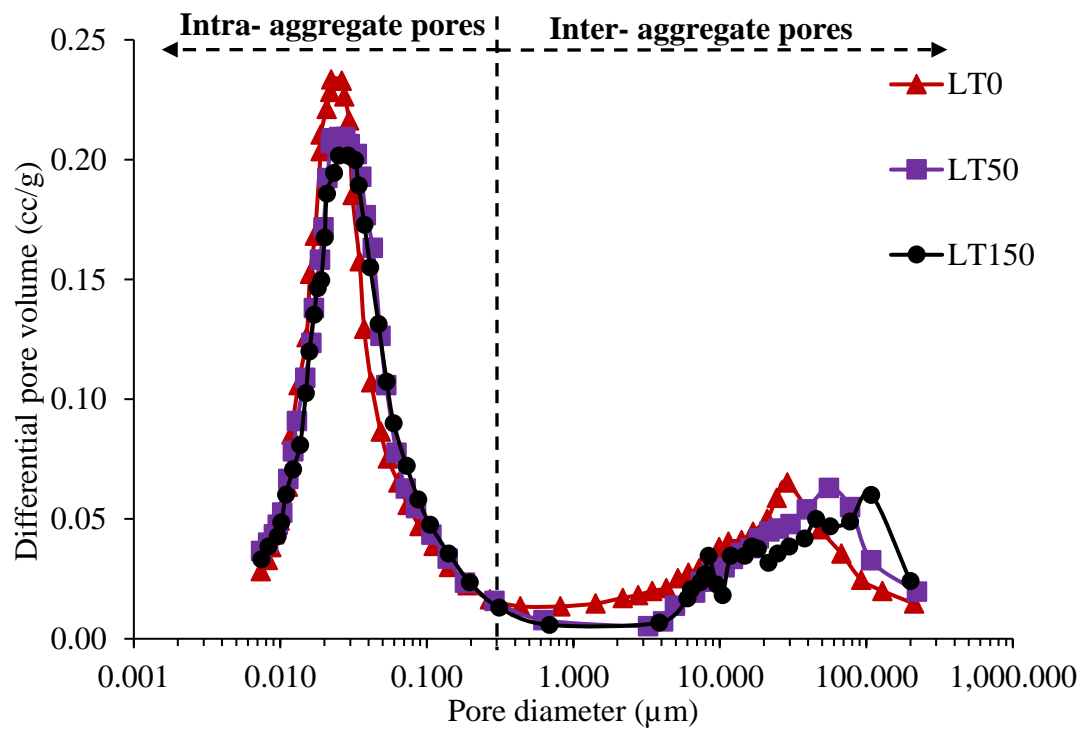


(c)

Fig. 9. SEM images of compacted lateritic sandy lean clay specimen at a) 150kPa suction, b) 50kPa suction and c) zero suction



(a)



(b)

Fig. 10. Pore size distribution of the lateritic specimen at various suction during wetting (a) cumulative intrusion void ratio and (b) pore size density function

Table 1. Classification and mineral composition of LAT tested in this study

Index test	Lateritic soil
Standard compaction Test	
Maximum dry density: kg/m <sup>3</sup>	1696
Optimum water content: %	20
Grain size distribution	
Percentage of sand: %	42
Percentage of silt: %	16
Percentage of clay: %	42
Coefficient of uniformity	35
Coefficient of gradation	1.6
Atterberg limits	
Liquid limit: %	44
Plastic limit: %	24
Plasticity index: %	20
Specific gravity	2.67
Soil classification based on USCS (ASTM,2011)	CL (sandy lean clay)
Chemical composition (%)	
Silicon oxide (SiO <sub>2</sub> )	60
Iron oxide (Fe <sub>2</sub> O <sub>3</sub> )	10
Aluminum oxide ( Al <sub>2</sub> O <sub>3</sub> )	28
Sesquioxide (Fe <sub>2</sub> O <sub>3</sub> + Al <sub>2</sub> O <sub>3</sub> ) content	Lateritic soil = 38%

Table 2. Details of test program

Series	Specimen ID	Matric suction: kPa	Net Confining pressure: kPa	Initial void ratio	Before consolidation		After consolidation		
					Water content (w)	Degree of saturation (Sr)	Void ratio	Degree of saturation (Sr)	Water content (w)
I <sup>a</sup>	LT0	0	20-400	0.653	0.24	0.98	N.A.		
	LT50	50		0.652	0.21	0.87	N.A.		
	LT150	150		0.653	0.19	0.79	N.A.		
II <sup>b</sup>	LT0-50	0	50	0.650	0.24	0.98	0.620	0.98	0.23
	LT50-50	50		0.652	0.20	0.87	0.635	0.87	0.21
	LT150-50	150		0.653	0.19	0.79	0.642	0.79	0.19
	LT0-100	0	100	0.650	0.24	0.98	0.609	0.99	0.23
	LT50-100	50		0.653	0.21	0.87	0.623	0.89	0.21
	LT150-100	150		0.652	0.19	0.79	0.629	0.83	0.19
	LT0-200	0	200	0.650	0.24	0.98	0.553	0.99	0.23
	LT50-200	50		0.654	0.21	0.87	0.582	0.91	0.21
	LT150-200	150		0.653	0.19	0.79	0.572	0.89	0.19

<sup>a</sup> Isotropic compression test; <sup>b</sup> Constant suction shearing

Table 3. Values of compressibility and strength parameters for LAT

s: kPa	$\lambda(s)$	N(s)	M(s)	$\mu(s)$ : kPa
0	0.073	1.78	1.56	0
50	0.070	1.82	1.58	25
150	0.143	2.01	1.57	50

Table 4. Details of MIP results

Specimen ID	Total void ratio	Intruded void ratio $e_{MIP}^*$	Intruded inter-aggregate void ratio	Intruded intra-aggregate void ratio
LT150	0.653	0.525	0.153	0.372
LT50	0.636	0.545	0.176	0.369
LT0	0.615	0.591	0.244	0.347